Characterization of LaMnAl$_{11}$O$_{19}$ by FT-IR spectroscopy of adsorbed NO and NO/O$_2$

M. Kantcheva [a,*], A. Agiral [a], O. Samarskaya [a], M. Stranzenbach [b], B. Saruhan [b]

[a] Department of Chemistry, Bilkent University, 06800 Bilkent, Ankara, Turkey
[b] DLR German Aerospace Center, Institute of Materials Research, 51170 Cologne, Germany

Abstract

The nature of the NO$_x$ species produced during the adsorption of NO at room temperature and during its coadsorption with oxygen on LaMnAl$_{11}$O$_{19}$ sample with magnetoplumbite structure obtained by a sol–gel process has been investigated by means of in situ FT-IR spectroscopy. The adsorption of NO leads to formation of anionic nitrosyls and/or *cis*-hyponitrite ions and reveals the presence of coordinatively unsaturated Mn^{3+} ions. Upon NO/O$_2$ adsorption at room temperature various nitro–nitrato structures are observed. The nitro–nitrato species produced with the participation of electrophilic oxygen species decompose at 350 °C directly to N$_2$ and O$_2$. No NO decomposition is observed in absence of molecular oxygen. The adsorbed nitro–nitrato species are inert towards the interaction with methane and block the active sites (Mn^{3+} ions) for its oxidation. Noticeable oxidation of the methane on the NO$_{x^-}$-precovered sample is observed at temperatures higher than 350 °C due to the liberation of the active sites as a result of decomposition of the surface nitro–nitrato species. Mechanism explaining the promoting effect of the molecular oxygen in the NO decomposition is proposed.
© 2005 Elsevier B.V. All rights reserved.

1. Introduction

Nitrogen oxides (NO$_x$), the byproducts of high-temperature fuel combustion, are dangerous atmo-spheric pollutants, which contribute to a variety of environmental problems. Among the various technologies for abatement of NO$_x$, catalytic fuel combustion and catalytic removal of NO$_x$ offer the most useful approaches. The unique thermal properties of the hexaaluminates make these materials one of the most promising candidates for the former process [1–3]. The high thermal stability of the hexaaluminates is

* Corresponding author. Tel.: +90 312 290 2451;
fax: +90 312 266 4579.
E-mail address: margi@fen.bilkent.edu.tr (M. Kantcheva).

associated with their layered structure consisting of spinel blocks separated by mirror planes on which large cations (Ba, Ca, La and Sr) are positioned [4]. The ionic radius and the oxidation state of the large cations determine the type of the crystal structure for the hexaaluminate (β-alumina or magnetoplumbite). The introduction of various transition metal ions (Cr, Mn, Fe, Co, Ni) enhances the combustion activity [4]. Among these La-containing Mn-substituted hexaaluminates of magnetoplumbite structure are the most active for methane combustion [2]. The crystallographic study [5] on $BaMn_xAl_{12-x}O_{19}$ samples revealed that at low manganese content (up to $x = 1$) manganese occupies the tetrahedral Al^{3+} sites as Mn^{2+}, whereas at higher concentration manganese(III) is located at the octahedral Al(III) sites. However, according to the TPR results reported by Groppi et al. [2] Mn^{3+} ions are found in the $LaMnAl_{11}O_{19}$, for which $x = 1$.

Due to their high thermal resistance, hexaaluminate systems may also be used as catalyst supports in the automotive catalytic converters [6]. In addition, transition-metal (Fe, Mn, Co, Ni, Cu) substituted haxaaluminogallates show activity for direct decomposition of NO in presence of oxygen [7]. The Co-, Ni- and Cu-containing materials catalyze the reduction of NO_x with propene in excess oxygen (40% NO conversion) [7]. It is proposed that in both processes surface nitrogen–oxygen complex is involved [7]. These results indicate that hexaaluminate-based compounds could be promising not only in the combustion but also in the post-combustion control of NO_x.

The object of the present work is (i) to identify by means of in situ FT-IR spectroscopy the species arising during the NO adsorption and its coadsorption with oxygen on the surface of $LaMnAl_{11}O_{19}$ catalyst obtained by a sol–gel method and (ii) to investigate the reactivity of strongly bound surface NO_x complexes toward methane. Results on the thermal stability and reactivity of strongly adsorbed NO_x species toward methane are also reported.

2. Experimental

2.1. Synthesis of sol–gel-derived powders

The synthesis procedure for lanthanum manganese hexaaluminate ($LaMnAl_{11}O_{19}$) sol is shown in Fig. 1.

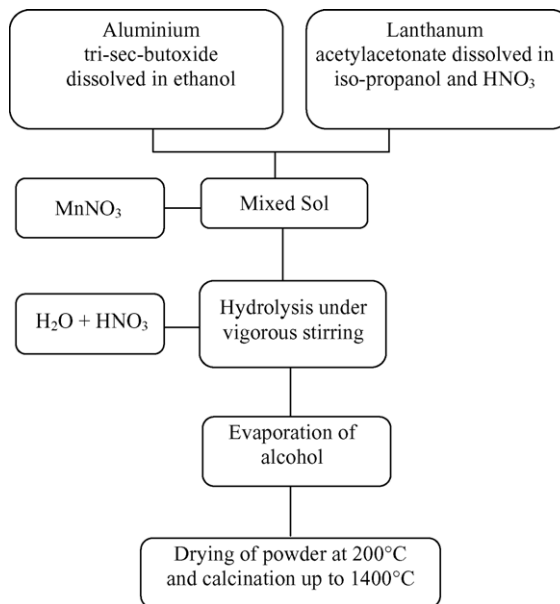Fig. 1. Flow chart showing the sol–gel synthesis of $LaMn_{11}O_{19}$ powder.

The starting materials were lanthanum acetate hydrate, $La(OOCCH_3)_3 \cdot 1.5H_2O$ (Alfa Aeser, Karlsruhe, Germany), aluminum tri-sec-butoxide $[CH_3CH_2(CH_3)O]_3Al$ (ABCR GmbH, Karlsruhe, Germany) and manganese(II) nitrate, 50% solution of $Mn(NO_3)_2$ (Alfa Aeser, Karlsruhe, Germany). Initially, lanthanum acetate was dissolved in ethanol and peptized with HNO_3 (60 mol/l solution) to obtain a clear sol at pH 6. Aluminum tri-sec-butoxide was mixed with 2-propanol and homogenized by stirring. Stoichiometric amount of lanthanum precursor sol was added to aluminum tri-sec-butoxide sol under vigorous stirring. The precursor solution mixture was cooled to room temperature into which stoichiometric amount of $Mn(NO_3)_2$ solution was added. This mixed sol was hydrolyzed by addition of distilled water until gelation. After evaporation of the alcohol in a rotary vaporizer, the $LaMnAl_{11}O_{19}$ powder was obtained. The powder was dried at 200 °C, before calcining at various temperatures from 600 to 1400 °C for 1 h.

2.2. Methods of characterization

Surface area of the powders calcined at 1000 °C was measured by BET using N_2 adsorption, which

yielded 15 m^2/g. After calcinations at about 1400 °C, the surface area was reduced to 10 m^2/g.

XRD measurements were carried out on a Siemens D 5000 diffractometer over scattering angles of $2\theta = 10$ to 80° using nickel-filtered Cu Kα radiation with a step size of 0.020° 2θ and a counting time of 10 s per step. The samples were characterized microstructurally and compositionally by scanning electron microscope (SEM) and energy dispersive X-ray spectroscopy (EDS) (LEITZ LEO 982, Germany). Other compositional determinations were carried out by an X-ray fluorescence analyzer (XRF) (Oxford MESA 5000, Germany). DR-UV–vis spectrum was obtained under ambient conditions with fiber optic spectrometer AvaSpec-2048 (Avantess) using WS-2 as a reference.

The FT-IR spectra were recorded on a Bomem MB 102 FT-IR spectrometer equipped with a liquid–nitrogen cooled MCT detector at a resolution of 4 cm^{-1} (128 scans). For the in situ FT-IR measurements a sample of the hexaaluminate calcined at 1000 °C for 1 h was used. The self-supporting discs were activated in the IR cell by heating for 1 h in vacuum at 500 °C and in oxygen (100 Torr, passed through a trap cooled in liquid nitrogen) at the same temperature, followed by evacuation for 1 h at 500 °C. A specially designed absorption IR cell (Xenonum Scientific SVCS, LLC, USA) equipped with BaF$_2$ windows allowed recording of the spectra at elevated temperatures. The sample holder of the cell can be moved up and down relative to the light beam, which gives the possibility for subtraction of the gas phase spectrum when needed.

The spectrum of the activated sample (taken at ambient temperature) was used as a background reference. It contains weak bands at 1505, 1411 and 1180 cm^{-1} due to residual carbonates. No absorption in the OH stretching region has been detected.

The purity of NO gas was 99.9% (air products).

3. Results and discussion

3.1. Compositional determination

La-hexaluminates forms highly defective magnetoplumbite crystal structure. Such a structure consists of $[AlO_{16}]^+$ spinel blocks intercalated by mirror planes of composition $[LaAlO_3]^0$. This composition results in an electrically charged cell $[LaAl_{12}O_{19}]^+$. Introduction of divalent ions such as Mn in the spinel blocks, replacing Al^{3+}, effectively compensates charge and yield electrically neutral structure and promotes the formation of magnetoplumbite phase, likely by increasing ion mobility in the γ-Al_2O_3 spinel blocks.

XRD analysis of powders of $LaMnAl_{11}O_{19}$ calcined at temperatures between 800 and 1200 °C shows that the as-received powder is amorphous up to 900 °C and crystallizes to magnetoplumbite phase at about 1000 °C after 1 h of heat-treatment (Fig. 2). As shown in Table 1, compared with the $LaAl_{11}O_{18}$, the crystallization of the $LaMnAl_{11}O_{19}$ powder to magnetoplumbite phase occurs directly and at lower temperatures [8,9]. It was observed [7,10] that in the non-doped powders crystallization to magnetoplumbite phase occurs after formation of intermediate phases such as γ-Al_2O_3 and
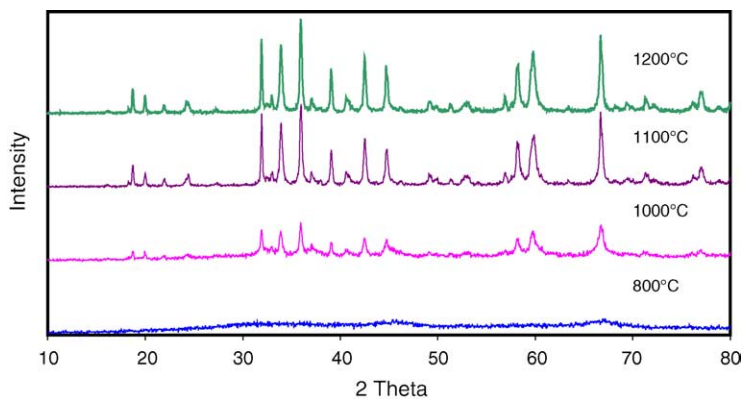

Fig. 2. X-ray diffractograms of the LaMn$_{11}$O$_{19}$ powders calcined at 600, 1000, 1100 and 1200 °C.

Table 1
Phase development at the manganese(II) doped and non-doped lanthanum hexaaluminates

Heat-treatment temperature (°C)	Phase(s)	
	$LaAl_{11}O_{18}$	$LaMnAl_{11}O_{19}$
500	Amorphous	Amorphous
900	γ-AlO_3	Amorphous
1000	γ-AlO_3	MP
1100	$LaAlO_3$	MP
1300	MP, $LaAlO_3$	MP
1400	MP	MP

$LaAlO_3$. Because of this fact, it can be assumed that magnetoplumbite phase formation in $LaAl_{11}O_{18}$ powder is due to a transformation reaction rather than crystallization, whereas doping with manganese(II) to obtain $LaMnAl_{11}O_{19}$ results in a crystallization process.

3.2. Microstructural observations

Scanning electron microscopy (SEM) investigation of the gelled and calcined powders (Fig. 3) shows the growth of plate-like hexagonal grains above about 1200 °C. After calcining above 1000 °C, the sol–gel synthesized $LaMnAl_{11}O_{19}$ powder shows a surface area reduction, which probably corresponds to the growth of plate-like grains. The growth of the grains is random and leads to an interlocking morphology.

3.3. DR-UV–vis spectroscopy

The electronic spectrum of the sample calcined at 1000 °C is shown in Fig. 4. According to the electronic configurations of Al^{3+} and La^{3+} no internal d-d transitions on these elements are expected. The spectrum displays features that are very similar to those reported for γ-Mn_3O_4 (hausmannite) [11]. This similarity is expected because of incorporation of the manganese ions in the spinel blocks of the magnetoplumbite structure. Based on the literature data [11], the bands at 240 and 260 nm are attributed to the allowed $O^{2-} \rightarrow Mn^{2+}$ charge transfer transitions. The remaining bands are assigned to $O^{2-} \rightarrow Mn^{3+}$ charge transfer transition (330 nm), superimposed $^5B_{1g} \rightarrow {}^5B_{2g}$ and $^5B_{1g} \rightarrow {}^5E_g$ crystal field d-d transitions (broad component at about 500 nm) and $^5B_{1g} \rightarrow {}^5A_{1g}$ crystal field d-d transition (weak band at 725 nm) of distorted octahedral Mn(III) [11]. The presence of Mn(III) is consistent with the higher oxidation state of manganese (2.17) in $LaMnAl_{11}O_{19}$ determined by Groppi et al. [2] from TPR experiments.

3.4. Adsorption of NO

The interaction of NO (30 Torr) with the surface of $LaMnAl_{11}O_{19}$ at room temperature (Fig. 5, spectrum (a)) gives number of different transformation species characterized by bands below 1650 cm^{-1}. According to the spectra of NO adsorbed on basic and amphoteric oxides such as MgO [12], La_2O_3 [13], ZrO_2 [14], TiO_2 [15], Al_2O_3 [16] and manganese-containing catalysts [15,16], the most reasonable assignment of the strong band at 1999 cm^{-1} with a shoulder at 1150 cm^{-1} is either to
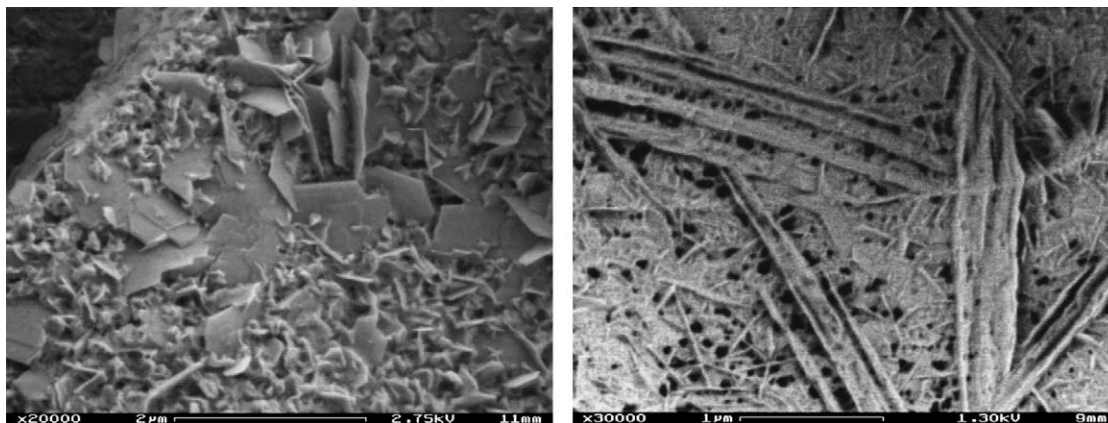

Fig. 3. Scanning electron micrographs of the $LaMn_{11}O_{19}$ powders after the calcination at 1400 °C.
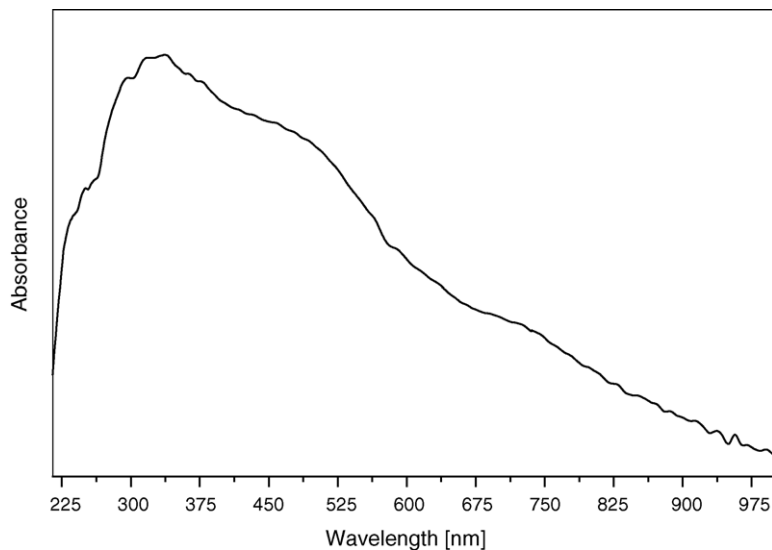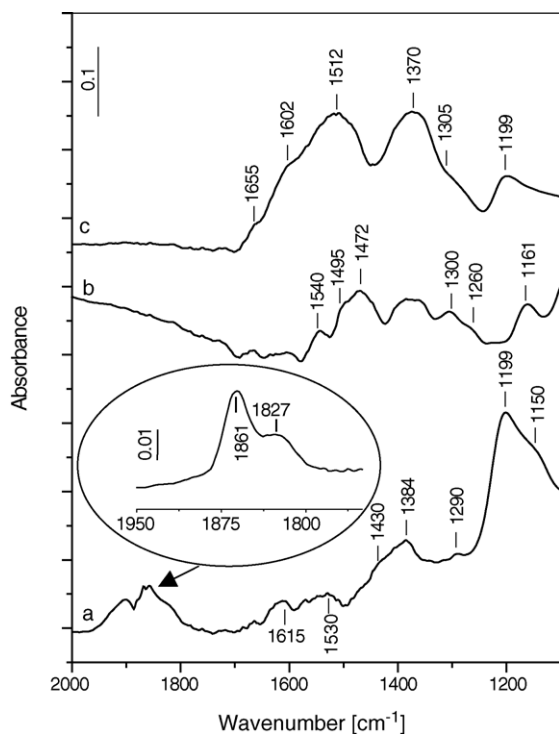
Fig. 4. DR-UV–vis spectrum of the sample calcined at 1000 °C.

Fig. 5. FT-IR spectra of NO (30 Torr) adsorbed on the activated LaMn$_{11}$O$_{19}$ sample for 20 min at room temperature (a), at 350 °C (b) and after cooling to room temperature (c). The inset shows the spectrum in the nitrosyl region after the subtraction of the gas phase spectrum. The spectrum of the activated sample is used as a background reference.

the ν(NO) stretching vibration of two types of anionic nitrosyls, NO$^-$, or the ν_s(NO) and ν_{as}(NO) modes of cis-hyponitrite ion, N$_2$O$_2^{2-}$, respectively. To the latter species the band at 1384 cm^{-1} (ν(N–N)) can be attributed. The weak band at 1615 cm^{-1} can be due to adsorbed NO$_2$, which usually appears as a byproduct during the formation of reduced species such as NO$^-$ and N$_2$O$_2^{2-}$ [15,16]. The bands at 1530 and 1290 cm^{-1} are assigned to the ν(N=O) and ν_{as}(NO$_2$) modes of bidentate nitrate species [13–15]. The unresolved absorption at about 1430 cm^{-1} could be due to the ν_{as}(NO$_2$) mode of monodentate and/or bridged nitro species [13–15]. In the nitrosyl region, after the subtraction of the spectrum of gaseous NO (see the inset in Fig. 5), two bands at 1861 and 1827 cm^{-1} are observed. As regards assignments of these bands, the following facts should be taken into account: (i) no linear nitrosyls on La^{3+} ions are reported [13], (ii) Al^{3+}–NO species are characterized by ν(NO) stretching mode at 1950–1985 cm^{-1} [16,17] and (iii) adsorption of NO at room temperature on manganese-containing oxide systems gives rise to absorption bands in the 1905–1830 cm^{-1} region attributed to Mn^{3+}–NO species [15,16] whereas the bands in the 1798–1760 cm^{-1} region correspond to Mn^{2+}–NO nitrosyls [15,18]. Based on these data and taking into account the electronic spectrum of the sample, it can be concluded that the bands at 1861 and 1827 cm^{-1}

are associated with manganese(III) species. It should be pointed out that in the case of NO adsorption on MnO_x/Al_2O_3 Kapteijn et al. [16] observed similar bands assigned to ν(NO) stretching modes of Mn^{3+}–NO species that is coordinatively saturated after NO adsorption (1865 cm^{-1}) and a species that still retains one coordinative unsaturation (1834 cm^{-1}). It can be proposed in the case of $LaMnAl_{11}O_{19}$ analogous Mn^{3+}–NO species are formed, which differ in the saturation of the coordination sphere of the manganese(III) adsorption sites. The intensity of the nitrosyl bands does not change upon prolonged NO adsorption (40 min).

Heating the sample at 350 °C for 20 min in NO atmosphere (Fig. 5, spectrum (b)) causes an increase in the intensities of the bands corresponding to the nitro–nitrate species and disappearance of the band with maximum at 1199 cm^{-1} due to the cis-$N_2O_2^{2-}$/NO^- ions. The band at 1161 cm^{-1} could be associated with the ν_s(NO$_2$) mode of two different bridged nitro species with ν_{as}(NO$_2$) stretching vibrations falling between 1420 and 1330 cm^{-1}. Lowering the temperature to room temperature leads to strong increase in the concentration of the surface nitro–nitrato structures (Fig. 5, spectrum (c)). The spectrum consists of intense unresolved bands indicating presence of surface nitrates tentatively assigned to bridged (1655 cm^{-1}), bidentate (1602 and 1512 cm^{-1}) and monodentate (1490 cm^{-1}) species. The shoulder at about 1305 cm^{-1} to the band with maximum at 1370 cm^{-1} (due to the nitro species) is attributed to the low-frequency component of the split ν_3 vibration of the nitrates. The strong increase in the amount of adsorbed nitro–nitrato species, which is observed after cooling to room temperature can be explained assuming oxidation of the adsorbed NO and cis-$N_2O_2^{2-}$/NO^- species by the Mn^{3+} ions at 350 °C. This is supported by the fact that after cooling to room temperature the manganese(III) nitrosyls are absent in the spectrum (Fig. 5, spectrum (c)). The presence of the band at 1199 cm^{-1} is associated with the reappearance of the cis-$N_2O_2^{2-}$/NO^- ions, however, with a concentration lower than that detected on the freshly activated sample (Fig. 5, spectrum (a)).

The anionic nitrosyl, NO^- and its dimmer, $N_2O_2^{2-}$, can form at room temperature on oxide surfaces by disproportionation of NO with involvement of the surface OH groups or O^{2-} as in the case of monoclinic zirconia, titania (anatase) and alumina [14–16]. As suggested for La_2O_3 [13], the adsorption of NO on single oxygen vacancy or pair of vacancies results also in reduced NO_x species. Since the sample after the activation at 500 °C is completely dehydroxylated, it is reasonable to assume that the anionic nitrosyls and/or hyponitrite ions are produced by the involvement of oxygen vacancies. These adsorption sites most probably participate in the formation of the NO_2^- (nitro) and NO_3^- species upon NO adsorption at room temperature on the freshly activated sample as well. This assumption is confirmed by the fact that the Mn^{3+}–NO nitrosyls are stable upon prolonged contact with NO indicating that oxidation of adsorbed NO by manganese(III) does not take place at room temperature. The oxygen vacancies can be created during the high-temperature activation of the sample.

In order to verify the role of the oxygen vacancies in the formation of the surface NO_x species, adsorption of NO on the activated sample left in contact with oxygen (100 Torr) for 30 min at room temperature followed by evacuation for 15 min has been performed. Fig. 6 compares the spectra of adsorbed NO on the activated catalyst (spectrum (a)) and on the sample treated with oxygen (spectrum (b)). The following noticeable differences are observed for the oxygen-preadsorbed sample:

 (i) Strong decrease in the amount of manganese(III) nitrosyls.
 (ii) Absence of the band at 1384 cm^{-1} and decrease in the intensity of the absorption at 1199 cm^{-1} (shifted to 1205 cm^{-1}). This is associated with decrease in the concentration or disappearance of the reduced species of adsorbed NO. Most probably, the band at 1205 cm^{-1} is due to both ν_s(NO) and ν_s(NO$_2$) stretching vibrations of cis-$N_2O_2^{2-}$ ion and bridged nitro species with the ν_{as}(NO$_2$) mode at 1430 cm^{-1}.
(iii) Formation of larger amount of surface nitrates (1606, 1544, 1520 and 1287 cm^{-1}).

These experimental facts indicate that the exposure of the activated sample to molecular oxygen at room temperature decreases the concentration of the oxygen vacancies and leads to formation of chemisorbed oxygen coordinated to Mn^{3+} ions, which is capable of oxidizing the reduced NO_x adsorption forms to surface nitrates.
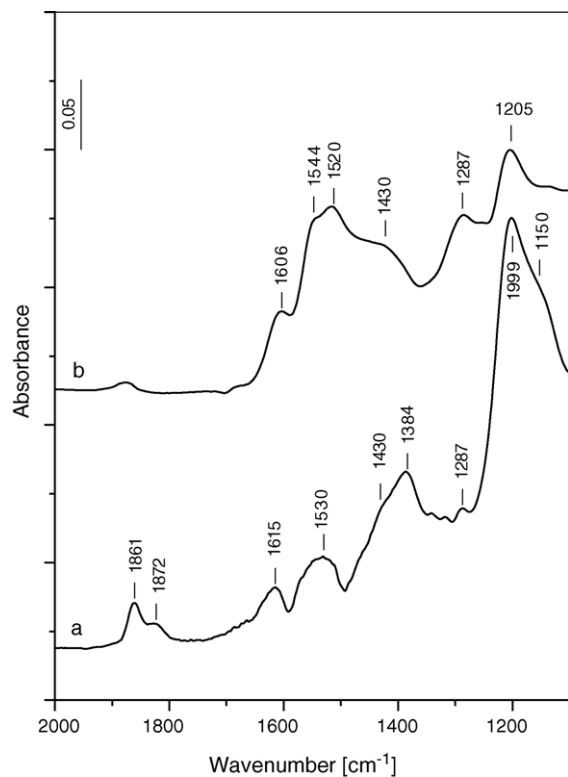
Fig. 6. FT-IR spectra of NO (30 Torr) adsorbed on the activated LaMn$_{11}$O$_{19}$ sample for 20 min at room temperature (a) and after adsorption of 100 Torr of O$_2$ at room temperature for 30 min followed by evacuation for 15 min (b). The spectrum of the activated sample is used as a background reference.

3.5. Coadsorption of NO and O$_2$

The addition of 60 Torr of oxygen to the IR cell (containing 30 Torr of NO) causes disappearance of the nitrosyl bands and drastic changes in the spectrum in the nitrite-nitrate region (Fig. 7A, spectrum (a)). The band at 1752 cm^{-1} is attributed to adsorbed N$_2$O$_4$. This indicates that gas-phase oxidation of NO has occurred. Indeed, the spectrum of the gas phase (the inset in Fig. 7A) contains very strong bands at 1755 and 1370 cm^{-1} due to the ν_9 and ν_1 modes of N$_2$O$_4$ [19]. The band at 1617 cm^{-1} (ν_3 mode) indicates presence of NO$_2$ with the ν_1 mode superimposed to the strong ν_1 band of N$_2$O$_4$. The weak absorption at 1876 cm^{-1} belongs to gaseous NO [19]. The adsorption of NO$_2$/N$_2$O$_4$, can take place by disproportionation with the participation of Lewis acid-base pairs

[20,21] leading to formation of surface nitrates (strong bands at 1640, 1566, 1516 and 1268 cm^{-1}) and NO$^+$ ions (ν(NO) at 2229 cm^{-1}). Since NO$_2$/N$_2$O$_4$ is strong oxidizing agent, it can be proposed that at room temperature oxidation of Mn^{3+} to Mn^{4+} can take place resulting in appearance of surface NO$_2^-$ (nitro) species (1450 and 1320 cm^{-1} [13–15]). On the other hand, upon NO/O$_2$ atmosphere, the chemisorption of O$_2$ on oxygen defect sites of the activated sample can lead to appearance of charged oxygen species such as O$_2^{2-}$ and O$^-$. They can be involved in the formation of adsorbed NO$_x$ species assuming for example the following reactions:

$$O_{(ads)}^- + NO_2 \rightarrow NO_3^- \tag{1}$$

$$O_{(ads)}^- + NO \rightarrow NO_2^- \tag{2}$$

The evacuation of the gas mixture for 15 min at room temperature causes little changes in the nitro–nitrate region and disappearance of the NO$^+$ and N$_2$O$_4$ bands. An attempt to assign the bands in the nitro–nitrato region was made investigating the thermal stability of the adsorbed NO$_x$ species. The spectra shown in Fig. 7B were obtained under vacuum treatment at elevated temperatures and recorded at room temperature. The changes in the shapes and the intensities of the nitrate bands observed under outgassing at 100 °C for 15 min indicate that rearrangement rather than decomposition of the NO$_3^-$ species has occurred. Noticeable decomposition of the surface NO$_x$ species begins at 175 °C. The evacuation for 15 min at 350 °C causes complete removal of the nitro–nitrate species. From the results of the thermal stability and the magnitude of the ν_3 spectral splitting [13–15] the nitrate bands are assigned to monodentate (1518 and 1292 cm^{-1}), bidentate (1571–1558 and 1268–1253 cm^{-1}) and bridged (1640 and 1269–1257 cm^{-1}) species. The bands at 1509, 1448 and 1306 cm^{-1}, which display high thermal stability, are attributed to NO$_2^-$ (nitro) species.

The results of heating the closed IR cell (without evacuation) containing the NO$_x$-precovered sample are shown in Fig. 8. The adsorbed NO$_x$ species were obtained at room temperature by addition of NO/O$_2$ mixture containing 30 Torr of NO and 60 Torr of oxygen for 20 min followed by evacuation for 30 min (Fig. 8, spectrum (a)). Keeping the sample for 20 min
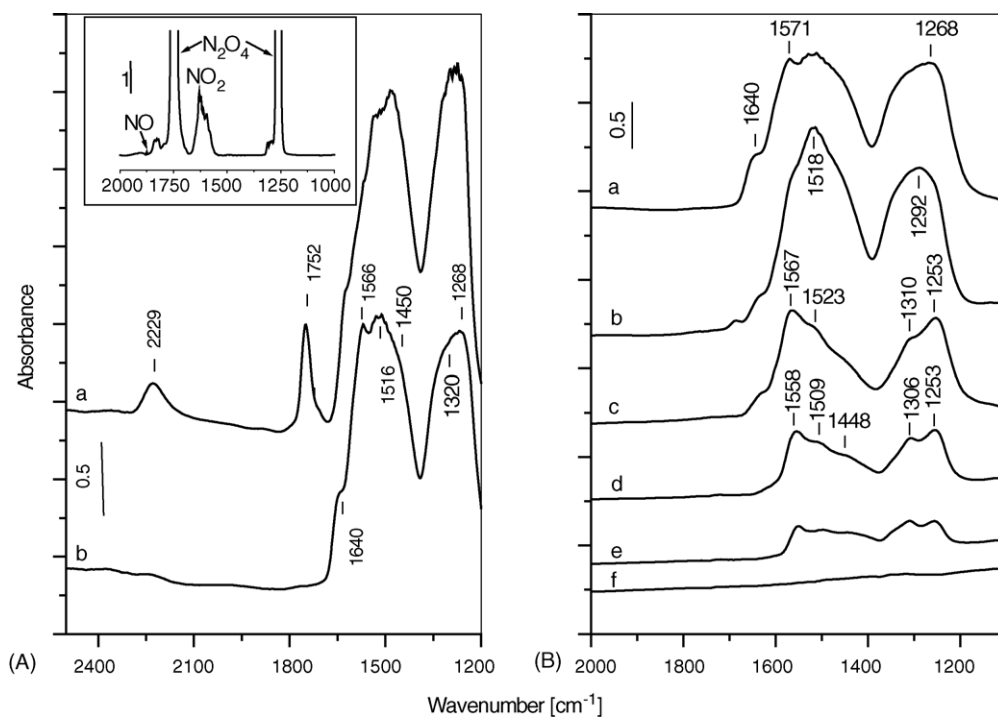
Fig. 7. (A) FT-IR spectra of adsorbed NO/O_2 mixture (90 Torr, $NO:O_2 = 1: 2$) at room temperature on the activated $LaMn_{11}O_{19}$ sample (a) and after evacuation for 15 min at room temperature (b) The inset in panel A shows the gas phase spectrum detected in the presence of NO/O_2 mixture. (B) FT-IR spectra obtained after heating the $LaMn_{11}O_{19}$ sample containing adsorbed NO_x species for 15 min in vacuum at: 100 °C (b), 175 °C (c), 250 °C (d), 300 °C (e) and 350 °C (f). The spectra are recorded after cooling the IR cell to room temperature. Spectrum (a) corresponds to spectrum (b) in panel A of the figure. The spectrum of the activated sample is used as a background reference.

at 350 °C causes strong decrease in the bands in the nitro–nitrato region (Fig. 8, spectrum (b)). The spectrum taken after cooling to room temperature (spectrum (c)) does not differ much from that at 350 °C. No NO and NO_2 have been detected in the gas phase. It can be assumed that the surface nitro–nitrato structures decompose upon heating to NO and/or NO_2 whose concentrations in the gas phase are low to be measured. The other possibility is that decomposition of the adsorbed NO_x species to N_2 and O_2 has occurred. In order to verify these assumptions a second portion of NO/O_2 mixture was added to the IR cell under the conditions described above (spectrum (a)). The resulting spectrum (d) is shown in Fig. 8. The shape of the bands in the nitro–nitrato region is identical to those obtained after the first admission of NO/O_2 mixture however with somewhat lower intensity. The spectrum (e) taken at 350 °C contains bands in the nitro–nitrato region with higher intensity than those observed after the first treatment at the same

temperature. This indicates that the amount of thermally stable NO_x species has increased. Spectrum (f) in Fig. 8 shows that the amount of NO_x species observed at room temperature is significantly higher than that in spectrum (c) taken at the same temperature after the first admission of NO/O_2 mixture. Based on these experimental facts it can be concluded that during the first heating at 350 °C the nitro–nitrato species formed on the freshly activated catalyst undergo decomposition to N_2 and O_2. This process occurs to a much smaller extent or not at all on the used hexaaluminate. After reactivation of the sample, the same cycle was again repeated and the same results were obtained.

Since the interaction of NO at 350 °C with the activated sample results in oxidation rather than its decomposition (see Fig. 5), it is reasonable to assume that the addition of oxygen promotes the decomposition of NO. At present we cannot propose unambiguous explanation of the observed effect. However, we
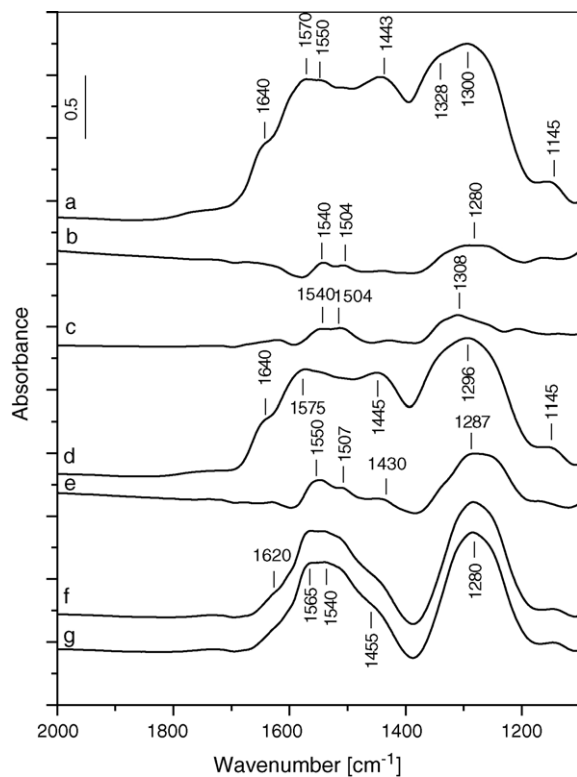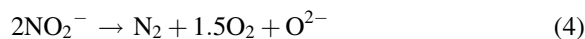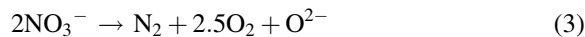
Fig. 8. FT-IR spectra of the $LaMn_{11}O_{19}$ sample taken after adsorption of NO/O_2 mixture (90 Torr, $NO:O_2 = 1:2$) for 20 min at room temperature followed by evacuation for 30 min (a), heating the closed IR cell for 20 min at 350 °C (b), and after cooling to room temperature (c), subsequent addition of a second NO/O_2 portion (90 Torr, $NO:O_2 = 1:2$) at room temperature followed by evacuation for 30 min (d), heating of the closed IR cell for 20 min at 350 °C (e), cooling to room temperature (f) and evacuation at room temperature for 15 min (g). The spectrum of the activated sample is used as a background reference.

assume that the surface nitro–nitrato species that are formed with involvement of electrophylic oxygen species (e.g. O^-, see reactions 1 and 2) can undergo decomposition at 350 °C according to the reactions:

$$2NO_3^- \rightarrow N_2 + 2.5O_2 + O^{2-} \tag{3}$$

$$2NO_2^- \rightarrow N_2 + 1.5O_2 + O^{2-} \tag{4}$$

As a result, the concentration of the oxygen defects decreases which leads to decrease in the amount of adsorbed nitro–nitrato species. Most probably, the nitro–nitrato species that appear during the second room-temperature adsorption of NO/O_2 are produced

predominantly by processes involving nucleophilic O^{2-} species. Upon heating, these NO_x structures follow different decomposition path evolving NO_2, which adsorbs at room temperature producing mainly NO_3^- species.

4. Reactivity toward methane

Heating of the activated sample at temperatures ranging from 300 to 450 °C for 15 min (Fig. 9, spectra (a)–(c)) in the presence of 45 Torr of methane leads to appearance of growing bands in the carbonate-carboxylate region. The bands at 1455 and 1378 cm^{-1} are attributed to the split ν_3 vibration of monodentate carbonates [15,22]. The weak absorptions at 2890, 2830 and 2575 cm^{-1} (see the inset in
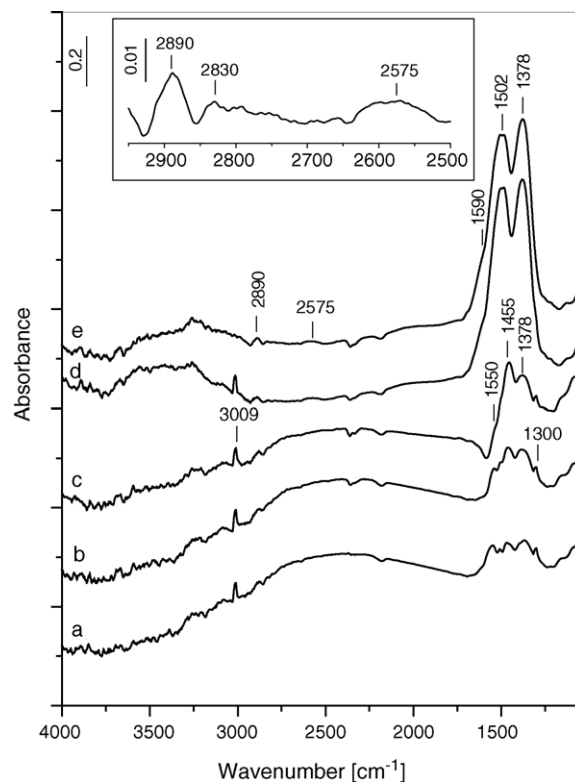

Fig. 9. FT-IR spectra of the $LaMn_{11}O_{19}$ sample taken after addition of methane (45 Torr) at room temperature followed by heating the closed IR cell for 20 min at 300 °C (a), 350 °C (b), 450 °C (c), after cooling to room temperature (d) and after evacuation for 10 min at room temperature (e). The spectrum of the activated sample is used as a background reference.

Fig. 8) together with the band at 1550 cm^{-1} are typical of formate species [15,22]. The former three bands are due to Fermi resonance between the ν(CH) fundamental and combinations or overtones of bands in the carboxylate region. The $\nu_{as}(CO_2)$ stretching vibration of the formate species is positioned at 1550 cm^{-1} whereas the δ(CH) frequency coincides with the low-frequency component of the split ν_3 vibration at 1378 cm^{-1} of the monodentate carbonates. The intensities of the carbonate-carboxylate bands increase significantly after cooling to room temperature (Fig. 9, spectrum (d)). All of the bands resist the room-temperature evacuation for 10 min (Fig. 9, spectrum (e)). The spectra taken under these conditions contain broad absorption in the 3750–2900 cm^{-1} region corresponding to adsorbed water molecules. These results indicate that the oxidation of methane takes place already at 300 °C. Since the experiment is performed in absence of molecular oxygen, the oxidation of the hydrocarbon is caused by oxide ions coordinated to the Mn^{3+} sites.

Fig. 10 shows the results on the reactivity of preadsorbed NO$_x$ compounds toward the methane at various temperatures. The surface NO$_x$ species are obtained by adsorption of NO/O$_2$ mixture (28 Torr, NO:O$_2$ = 1:2.5) for 20 min at room temperature followed by evacuation for 30 min. To the catalyst treated in this way, methane (45 Torr) is added (Fig. 10, spectrum (a)) and then the closed IR cell is heated for 15 min at various temperatures. The spectra are taken after cooling to room temperature. Heating at 250 and 350 °C causes strong decrease in the intensities of the nitro–nitrato bands. Based on the results discussed in the previous section, it can be concluded that this decrease is associated mainly with the decomposition of the nitro–nitrato structures to nitrogen rather than with their interaction with the methane (compare spectrum (c) in Fig. 10 with spectrum (c) in Fig. 8). Noticeable oxidation of the methane is achieved after heating at 450 °C. The spectrum taken after the evacuation for 10 min at room temperature (Fig. 10, spectrum (d)) contains a broad absorption in the ν(OH) stretching region and bands between 1650 and 1300 cm^{-1} associated with adsorbed water molecules and carbonate-carboxylate species (compare with spectrum (d) in Fig. 9). The fact that the oxidation of the methane on the NO$_x$-precovered catalysts is shifted to higher
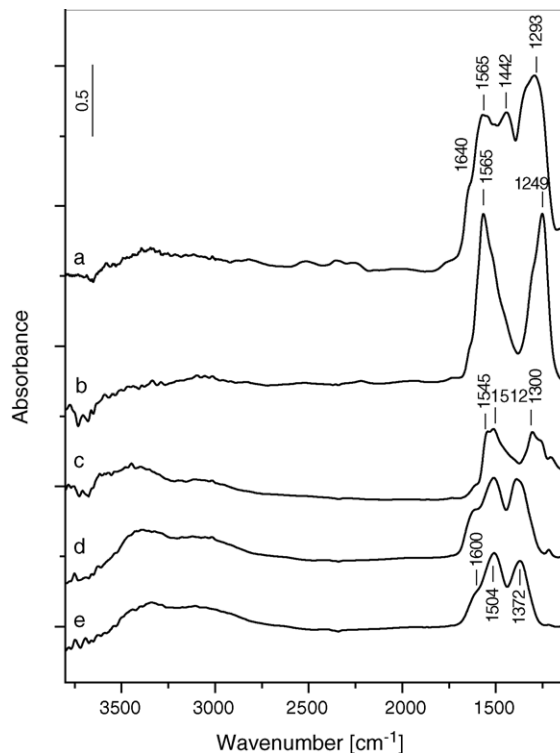

Fig. 10. FT-IR spectra of the LaMn$_{11}$O$_{19}$ sample taken after adsorption of NO/O$_2$ mixture (90 Torr, NO:O$_2$ = 1:2) at room temperature for 20 min followed by evacuation for 30 min and addition of 45 Torr of methane (a) and after heating the closed IR cell for 15 min at 250 °C (b), 350 °C (c), 450 °C. The spectra are recorded after cooling the IR cell to room temperature. Spectrum (e) is taken after evacuation for 10 min at room temperature. The spectrum of the activated sample is used as a background reference.

temperature (above 350 °C) compared to the NO$_x$-free catalyst (on which the oxidation of methane takes place already at 300 °C) indicates that the adsorbed nitro–nitrato species are unreactive and block the active sites for CH$_4$ oxidation. With an increasing temperature, the nitro–nitrato species undergo decomposition, thus liberating active sites for the oxidation of methane.

5. Conclusions

The adsorption of NO at room temperature on LaMnAl$_{11}$O$_{19}$ with magnetoplumbite structure leads to formation of anionic nitrosyls and/or *cis*-hyponitrite ions and reveals the presence of coordinatively

unsaturated Mn^{3+} ions. The reduced NO_x species are produced by the involvement of oxygen vacancies.

The coadsorption of NO and O_2 at room temperature on the sample studied leads to formation of various nitro–nitrato structures. The nitro–nitrato species formed with the participation of electrophilic oxygen species decompose at 350 °C directly to N_2 and O_2. No NO decomposition is observed in absence of molecular oxygen.

The interaction of methane with the surface of $MnLaAl_{11}O_{19}$ in absence of molecular oxygen occurs already at 300 °C. The adsorbed nitro–nitrato species are inert toward the methane oxidation and block the active sites (Mn^{3+} ions) of this process. Noticeable oxidation of the methane on the NO_x-precovered sample is observed at temperatures higher than 350 °C due to the liberation of the active sites as a result of decomposition of the surface nitro–nitrato species.

Acknowledgements

References

[1] K. Eguchi, H. Arai, Catal. Today 29 (1996) 379.
[2] G. Groppi, C. Cristiani, P. Forzatti, Appl. Catal. B 35 (2001) 137.
[3] P. Forzatti, Catal. Today 83 (2003) 3.
[4] M. Machida, K. Eguchi, H. Arai, J. Catal. 120 (1989) 377.
[5] M. Belloto, G. Artioli, C. Cristiani, P. Forzatti, G. Groppi, J. Catal. 179 (1998) 597.
[6] M. Machida, Y. Teshima, K. Eguchi, H. Arai, Chem. Lett. (1991) 231.
[7] T. Yamaguchi, W. Sakamoto, T. Yogo, Sh.-i. Hirano, J. Am. Ceram. Soc. 85 (2002) 909.
[8] B. Saruhan, L. Mayer, H. Schneider, in: N.P. Bansal, J.P. Singh (Eds.), Innovative Processing/Synthesis: Ceramics, Glasses, Composites II, Ceramic Transactions, vol. 94, The American Ceramic Society, Westerville, 1999, pp. 215–226.
[9] B. Saruhan, U. Schulz, C. Leyens, in: Proceedings of the 8th Conference on European Ceramic Society Key Engineering Materials, June, Trans Tech Publications Ltd., Uetikon-Zurich, Istanbul, Turkey, 2003.
[10] M.H. Han, Y.S. Ahn, S.K. Kim, S.K. Shon, S.K. Kang, S.J. Chon, Mat. Sci. Eng. A 302 (2001) 286.
[11] J. Boyero Macstre, E. Fernández López, J.M. Gallardo-Amores, R. Ruano Casero, V. Sánchez Escribano, E. Pérez Bernal, Int. J. Inorg. Mater. 3 (2001) 889.
[12] L. Cerruti, E. Modone, E. Guglielminotti, E. Berollo, J. Chem. Soc. Faraday Trans. I 70 (1974) 729.
[13] S.-J. Huang, A.B. Walters, M.A. Vannice, J. Catal. 192 (2000) 29.
[14] M. Kantcheva, E.Z. Ciftlikli, J. Phys. Chem. B 106 (2002) 3941.
[15] M. Kantcheva, J. Catal. 204 (2001) 479.
[16] K. Kapteijn, L. Singoredjo, M. van Driel, A. Andreini, J.A. Moulijn, G. Ramis, G. Busca, J. Catal. 150 (1994) 105.
[17] D.V. Pozdnyakov, V.N. Filimonov, Kinet. Katal. 14 (1973) 1020.
[18] A. Kuznetzov, I. Vorontzov, I. Miheilkin, Russ. J. Phys. Chem. 71 (1997) 1212.
[19] J. Laane, J.R. Ohlsen, Prog. Inorg. Chem. 28 (1986) 465.
[20] M. Kantcheva, V. Bushev, K. Hadjiivanov, J. Chem. Soc. Faraday Trans. 88 (1992) 3087.
[21] K. Hadjiivanov, V. Bushev, M. Kantcheva, D. Klissurski, Langmuir 10 (1994) 464.
[22] M. Kantcheva, M.U. Kucukkal, S. Suzer, J. Catal. 190 (2000) 144.